Inorganic Chemistry

Article

pubs.acs.org/IC

Unified View of Oxidative C−H Bond Cleavage and Sulfoxidation by a Nonheme Iron(IV)−Oxo Complex via Lewis Acid-Promoted Electron Transfer

Jiyun Park,[†] Yuma Morimoto,[†] Yong-Min Lee,[‡] Wonwoo Nam,*[,‡] and Shunichi Fukuzumi*[,†,‡]

[†]Department of Material and Life Science, Graduate School of Engineering, Osaka University, ALCA, Japan Science and Technology Agency (JST), Suita, Osaka 565-0871, Japan

[‡]Department of Chemistry and Nano Science, Department of Bioinspired Science, Ewha Womans University, Seoul 120-750, Korea

Supporting Information

ABSTRACT: Oxidative C−H bond cleavage of toluene derivatives and sulfoxidation of thioanisole derivatives by a nonheme iron(IV)−oxo complex, $[(N4Py)Fe^{IV}(O)]^{2+}$ (N4Py = *N*,*N*-bis(2-pyridylmethyl)-*N*-bis(2-pyridyl)methylamine), were remarkably enhanced by the presence of triflic acid (HOTf) and $Sc(OTf)_3$ in acetonitrile at 298 K. All the logarithms of the observed second-order rate constants of both the oxidative C−H bond cleavage and sulfoxidation reactions exhibit remarkably unified correlations with the driving forces of proton-coupled electron transfer (PCET) and metal ion-coupled electron transfer (MCET) in light of the Marcus theory of electron transfer when the differences in the formation constants of precursor complexes between PCET and MCET were taken into account, respectively. Thus, the mechanisms of both the oxidative C−H bond cleavage of toluene derivatives and sulfoxidation of thioanisole derivatives by $[(N4Py)Fe^{IV}(O)]^{2+}$ in the presence of HOTf and $Sc(OTf)_3$ have been unified as the rate-determining electron transfer, which is coupled with binding of $[(N4Py)Fe^{IV}(O)]^{2+}$ by proton (PCET) and $Sc(OTf)_3$ (MCET). There was no deuterium kinetic isotope effect (KIE) on the oxidative C−H bond cleavage of toluene via the PCET pathway, whereas a large KIE value was observed with $Sc(OTf)_3$, which exhibited no acceleration of the oxidative C−H bond cleavage of toluene. When HOTf was replaced by DOTf, an inverse KIE (0.4) was observed for PCET from both toluene and $[Ru^{II}(bpy)_3]^{2+}$ (bpy =2,2′-bipyridine) to $[(N4Py)Fe^{IV}(O)]^{2+}$. The PCET and MCET reactivities of $[(N4Py)Fe^{IV}(O)]^{2+}$ with Brønsted acids and various metal triflates have also been unified as a single correlation with a quantitative measure of the Lewis acidity.

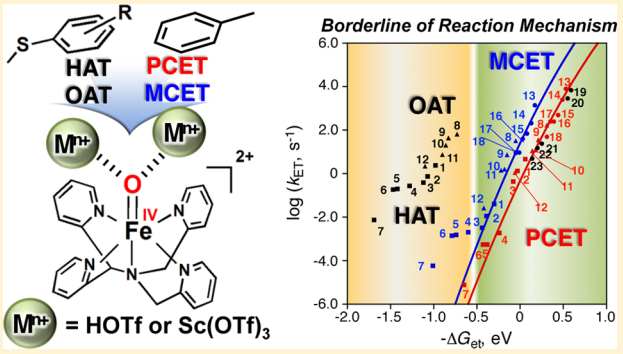

INTRODUCTION

High-valent heme and nonheme iron−oxo complexes have been investigated as key intermediate in various biological and chemical oxidation reactions.[1,2] Since the first crystal structure of mononuclear nonheme iron(IV)−oxo was reported in 2003, the reactivity of synthetic nonheme iron(IV)−oxo complexes with various substrates have been extensively studied.[3−17] Reactivities of nonheme iron(IV)−oxo complexes in various oxidation reactions, such as oxidative C−H bond cleavage and oxygen atom transfer, are significantly affected not only by axial ligand and solvents,[3−21] but also by binding of metal ions (Lewis acids) and Brønsted acids to the oxo moiety of nonheme iron(IV)−oxo complexes.[22−26] The binding of $Sc(OTf)_3$ to a nonheme iron(IV) complex was confirmed by the X-ray crystal structure of $Sc(OTf)_3$-bound $[(TMC)Fe^{IV}(O)]^{2+}$ (TMC = 1,4,8,11-tetramethyl-1,4,8,11-tetraazacyclotetradecane).[23,24] The electron transfer (ET) reactivity of a nonheme iron(IV)−oxo complex ($[(N4Py)Fe^{IV}(O)]^{2+}$) with electron donors was enhanced by binding of protons and metal ions, and the enhanced reactivity was well analyzed in light of the Marcus theory of electron transfer.[26] The enhanced reactivity of $[(N4Py)Fe^{IV}(O)]^{2+}$ in the oxidative C−H bond cleavage of toluene derivatives and sulfoxidation of thioanisole derivatives by acids is suggested to result from the change in the reaction mechanism from the direct hydrogen atom transfer and oxygen atom transfer to electron transfer pathways coupled with binding of acids to $[(N4Py)Fe^{IV}(O)]^{2+}$, respectively. If this is true, all the rate constants of oxidative C−H bond cleavage and sulfoxidation reactions as well as electron-transfer reactions in the absence and presence of acids would be correlated by a unified fashion to the corresponding driving force of electron transfer in light of the Marcus theory of electron transfer. However, such unified understanding of the reactivity of nonheme iron(IV)−oxo complexes in various oxidation reactions has yet to be made. In addition, unified understanding of effects of various acids (Brønsted and Lewis acids) on the

Received: December 21, 2013
Published: March 7, 2014

   dx.doi.org/10.1021/ic403124u | *Inorg. Chem.* 2014, 53, 3618−3628

reactivity of nonheme iron(IV)−oxo complexes has not been made, either.

We report herein a unified view on the remarkable enhancement of reactivity of $[(N4Py)Fe^{IV}(O)]^{2+}$ by triflic acid (HOTf) as well as $Sc(OTf)_3$ in oxidative C−H bond cleavage and oxygen atom transfer reactions as well as electron transfer from various one-electron donors to $[(N4Py)Fe^{IV}(O)]^{2+}$ in light of the Marcus theory of electron transfer. All the rate constants of oxidative C−H bond cleavage of toluene derivatives, sulfoxidation of thioanisole derivatives and electron transfer from various one-electron donors to $[(N4Py)Fe^{IV}(O)]^{2+}$ in the presence of HOTf and $Sc(OTf)_3$ are well correlated by a unified fashion with the driving forces of proton-coupled electron transfer (PCET) and metal ion ($Sc(OTf)_3$)-coupled electron transfer (MCET), respectively. In this paper, PCET and MCET are defined as electron-transfer reactions, which occur by binding of protons and metal ions to electron acceptors, respectively.[27] The enhanced reactivities of $[(N4Py)Fe^{IV}(O)]^{2+}$ with HOTf and $M^{n+}(OTf)_n$ are also well correlated with a quantitative measure of the Lewis acidity of acids, which we reported previously.[23b]

EXPERIMENTAL SECTION

Materials. All chemicals, which were the best available purity, were purchased from Aldrich Chemical Co. and Tokyo Chemical Industry and used without further purification unless otherwise noted. Solvents, such as acetonitrile (MeCN) and diethyl ether, were dried according to the literature procedures and distilled under Ar prior to use.[28] A nonheme iron(II) complex, $[(N4Py)Fe^{II}(MeCN)](ClO_4)_2$, and its corresponding iron(IV)−oxo complex, $[(N4Py)Fe^{IV}(O)]^{2+}$, were prepared by literature methods.[19,29] Iodosylbenzene (PhIO) was prepared by a literature method.[30] Triflic acid was purchased from Tokyo Chemical Industry. $[Fe^{II}(Ph_2phen)_3](PF_6)_2$ (Ph_2phen = 4,7-diphenyl-1,10-phenanthroline), $[Fe^{II}(Clphen)_3](PF_6)_2$ (Clphen = 5-chloro-1,10-phenanthroline), $[Ru^{II}(4,4'\text{-}Me_2bpy)_3](PF_6)_2$ (4,4′-Me_2bpy = 4,4′-dimethyl-2,2′-bipyridine), $[(Ru^{II}(5,5'\text{-}Me_2bpy)_3](PF_6)_2$ (5,5′-Me_2bpy = 5,5′-dimethyl-2,2′-bipyridine), $[Ru^{II}(bpy)_3](PF_6)_2$ and $[Ru^{II}(NO_2phen)_3](PF_6)_2$ (NO_2phen = 5-nitro-1,10-phenanthroline) were prepared according to published procedures.[31] $[Fe^{II}(bpy)_3](PF_6)_2$ was obtained by the addition of an aqueous solution containing an excess amount of $NaPF_6$ to an aqueous solution containing a stoichiometric amount of the bpy ligand and $FeSO_4$ to yield crystalline solids.

Kinetic Studies. Kinetic measurements were performed on a Hewlett-Packard 8453 photodiode-array spectrophotometer using a quartz cuvette (path length = 10 mm) at 298 K. The C−H bond cleavage of toluene derivatives and sulfoxidation of thioansiole derivatives by $[(N4Py)Fe^{IV}(O)]^{2+}$ were monitored by spectral changes at 695 nm due to $[(N4Py)Fe^{IV}(O)]^{2+}$ (2.5×10^{-4} M) with various concentrations of toluene and thioanisole derivatives (2.5×10^{-3}−1.0×10^{-1} M) in the absence and presence of acids, HOTf and $Sc(OTf)_3$, in MeCN at 298 K. The rates of the oxidation reactions of organic substrates by $[(N4Py)Fe^{IV}(O)]^{2+}$ were monitored by the decay of the absorption band at 695 nm due to $[(N4Py)Fe^{IV}(O)]^{2+}$ (λ_{max} = 695 nm) in the absence and presence of HOTf and $Sc(OTf)_3$ in MeCN. The concentrations of toluene derivatives and thioanisole derivatives were maintained at least more than 10-fold excess of $[(N4Py)Fe^{IV}(O)]^{2+}$ to attain pseudo-first-order conditions.

ET from electron donors to $[(N4Py)Fe^{IV}(O)]^{2+}$ in the presence of Lewis acids, HOTf and $Sc(OTf)_3$, was monitored by a Hewlett-Packard 8453 photodiode-array spectrophotometer and a UNISOKU RSP-601 stopped-flow spectrometer equipped with a MOS-type highly sensitive photodiode array in MeCN at 298 K. These ET rates were determined from the decay of $[(N4Py)Fe^{IV}(O)]^{2+}$ (λ_{max} = 695 nm), respectively. All kinetic measurements were carried out under pseudo-first-order conditions where the concentrations of electron donors were maintained to be in excess more than 10-fold of that of $[(N4Py)Fe^{IV}(O)]^{2+}$.

First-order fitting of the kinetic data allowed us to determine the pseudo-first-order rate constants. The first-order plots were linear for three or more half-lives with the correlation coefficient $\rho > 0.999$. In each case, it was confirmed that the rate constants derived from at least five independent measurements agreed within an experimental error of ±5%. The pseudo-first-order rate constants increased proportionally with increase in concentrations of substrates, from which second-order rate constants were determined.

Spectral Redox Titration. ET from an electron donor ($[Ru^{II}(NO_2phen)_3](PF_6)_2$ (2.5×10^{-4}−1.0×10^{-3} M)) to $[(N4Py)Fe^{IV}(O)]^{2+}$ (2.5×10^{-4} M) was examined by the spectral change in the presence of HOTf (1.0×10^{-2} M) in MeCN at 298 K using a Hewlett-Packard 8453 photodiode array spectrophotometer with a quartz cuvette (path length = 10 mm).

Product Analysis. Typically, hexamethylbenzene and thioanisole (2.0×10^{-2} M) were added to an MeCN solution containing $[(N4Py)Fe^{IV}(O)]^{2+}$ (4.0×10^{-3} M) in the presence of HOTf and $Sc(OTf)_3$ (1.0×10^{-2} M) in a vial. Products formed in the oxidation reactions of toluene derivatives by $[(N4Py)Fe^{IV}(O)]^{2+}$, which were carried out in the presence of acids under Ar atmosphere in MeCN-d_3 at 298 K, were analyzed by ^{1}H NMR. Quantitative analyses were made on the basis of comparison of ^{1}H NMR spectral integration between products and their authentic samples.

Instrumentation. The EPR spectra were measured with a JEOL X-band spectrometer (JES-RE1XE). The EPR spectra were recorded under nonsaturating microwave power conditions. The magnitude of modulation was chosen to optimize the resolution and the signal-to-noise (S/N) ratio of the observed spectra. The g value was calibrated by using a Mn^{2+} marker. ^{1}H NMR spectra were recorded on a JEOL A-300 spectrometer in MeCN-d_3.

RESULTS AND DISCUSSION

HOTf- and $Sc(OTf)_3$-Promoted C−H Bond Cleavage of Toluene Derivatives by $[(N4Py)Fe^{IV}(O)]^{2+}$. Toluene is known to be hardly oxidized by nonheme iron(IV)−oxo complexes.[19] However, oxidation of toluene by a nonheme iron(IV)−oxo complex ($[(N4Py)Fe^{IV}(O)]^{2+}$) in acetonitrile (MeCN) is significantly enhanced by the presence of HOTf (50 mM) as shown in Figure 1, to yield benzyl alcohol and $[(N4Py)Fe^{III}]^{3+}$ (eq 1);

$$PhCH_3 + 2[(N4Py)Fe^{IV}(O)]^{2+} + 2H^+ + H_2O \rightarrow PhCH_2OH + 2[(N4Py)Fe^{III}(OH_2)]^{3+} \quad (1)$$

see Figures S1−S3 in Supporting Information (SI). The $[(N4Py)Fe^{IV}(O)]^{2+}$ complex acted as a one-electron oxidant, when the yield of benzyl alcohol in the presence of HOTf was 50% based on $[(N4Py)Fe^{IV}(O)]^{2+}$ (Figure S1 in SI). Other toluene derivatives were also oxidized by $[(N4Py)Fe^{IV}(O)]^{2+}$ in the presence of HOTf to produce the alcohol products with the maximum yield of 50%.

The rate of oxidation of toluene $[(N4Py)Fe^{IV}(O)]^{2+}$ in the absence and presence of HOTf in MeCN, monitored by decrease in absorbance at 695 nm due to $[(N4Py)Fe^{IV}(O)]^{2+}$ (Figure 1) obeyed first-order kinetics (Figure S4 in SI) with a large excess of toluene and HOTf. The pseudo-first-order rate constant (k_f) increased linearly with increasing concentration of toluene (Figure S5a in SI). Similarly the k_f values were also proportional to concentrations of toluene derivatives (Figures S5b−S5f in SI). The observed second-order rate constants (k_{obs}) of oxidation of toluene derivatives by $[(N4Py)Fe^{IV}(O)]^{2+}$ were determined from the slopes of plots of k_f vs concentrations of toluene derivatives in the absence and

dx.doi.org/10.1021/ic403124u | Inorg. Chem. 2014, 53, 3618−3628

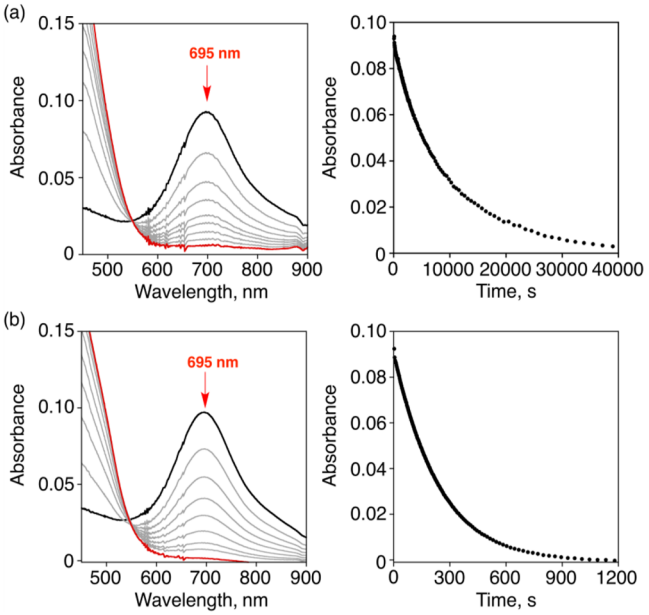

Figure 1. Visible spectral changes observed in the reactions of $[(N4Py)Fe^{IV}(O)]^{2+}$ (0.25 mM) with toluene (400 mM) in the (a) absence and (b) presence of 50 mM of HOTf in MeCN at 298 K (left panel). Right panels show the time course of absorbance monitored at 695 nm due to the decay of $[(N4Py)Fe^{IV}(O)]^{2+}$.

presence of HOTf (10 mM) in MeCN at 298 K as listed in Table 1.

The k_{obs} values increased with increasing concentration of HOTf, [HOTf], exhibiting first-order and second-order dependence on [HOTf] at lower and higher concentrations of HOTf, respectively, as given by eq 2 (Figure 2),

$$k_{obs} = k_0 + [HOTf](k_1 + k_2[HOTf]) \quad (2)$$

$$(k_{obs} - k_0)/[HOTf] = k_1 + k_2[HOTf] \quad (3)$$

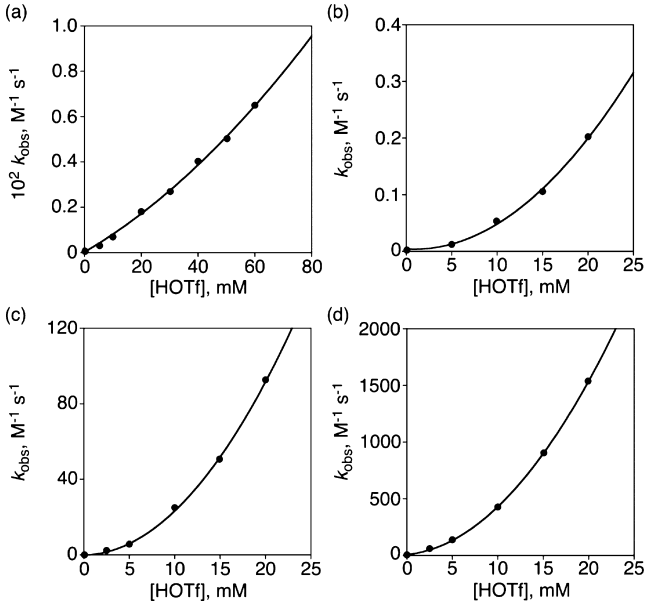

Figure 2. Plots of k_{obs} vs concentration of HOTf for oxidation of toluene derivatives [(a) toluene, (b) 1,3,5-trimethylbenzene, (c) 1,2,4,5-tetramethylbenzene and (d) hexamethylbenzene] by $[(N4Py)Fe^{IV}(O)]^{2+}$ in the presence of HOTf in MeCN at 298 K.

Table 1. One-Electron Oxidation Potentials (E_{ox}) of Toluene and Thioanisole Derivatives and Second-Order Rate Constants of the C−H Bond Cleavage and Sulfoxidation by $[(N4Py)Fe^{IV}(O)]^{2+}$ in the Presence of HOTf and $Sc(OTf)_3$ (10 mM) in MeCN at 298 K

			k_{obs}, $M^{-1}\ s^{-1}$		
no.	thioanisole and toluene derivative	E_{ox} (vs SCE, V)[a,b]	without acid[a,b]	with $Sc(OTf)_3$ (10 mM)	with HOTf (10 mM)[e]
1	hexamethylbenzene	1.49	$(4.8 \pm 0.2) \times 10^{-2}$	$(1.1 \pm 0.1) \times 10^{-1}$	$(4.2 \pm 0.2) \times 10^{2}$
2	1,2,3,4,5-pentamethylbenzene	1.58	$(1.5 \pm 0.1) \times 10^{-2}$	$(2.9 \pm 0.1) \times 10^{-2}$	$(1.2 \pm 0.1) \times 10^{2}$
3	1,2,4,5-tetramethylbenzene	1.63	$(7.8 \pm 0.4) \times 10^{-3}$	$(1.1 \pm 0.1) \times 10^{-2}$	$(3.9 \pm 0.2) \times 10$
4	1,2,4-trimethylbenzene	1.79	$(5.5 \pm 0.2) \times 10^{-3}$	$(8.2 \pm 0.4) \times 10^{-3}$	$(1.7 \pm 0.1) \times 10^{-1}$
5	1,4-dimethylbenzene	1.93	$(4.0 \pm 0.1) \times 10^{-3}$	$(6.0 \pm 0.3) \times 10^{-3}$	$(5.0 \pm 0.2) \times 10^{-2}$
6	1,3,5-trimethylbenzene	1.98	$(3.7 \pm 0.1) \times 10^{-3}$	$(5.6 \pm 0.3) \times 10^{-3}$	$(5.0 \pm 0.2) \times 10^{-2}$
7	toluene	2.20	$(1.5 \pm 0.1) \times 10^{-4}$	$(2.4 \pm 0.2) \times 10^{-4}$	$(6.5 \pm 0.2) \times 10^{-4}$
8	*p*-Me-thioanisole	1.24	1.3 ± 0.1	$(8.4 \pm 0.4) \times 10^{a}$	$(1.5 \pm 0.1) \times 10^{4}$
9	thioanisole	1.34	$(8.7 \pm 0.4) \times 10^{-1}$	$(1.9 \pm 0.1) \times 10^{a}$	$(3.2 \pm 0.2) \times 10^{3}$
10	*p*-Cl-thioanisole	1.37	$(4.0 \pm 0.2) \times 10^{-1}$	4.2 ± 0.2^{a}	$(1.1 \pm 0.1) \times 10^{3}$
11	*p*-Br-thioanisole	1.41	$(1.5 \pm 0.1) \times 10^{-1}$	3.7 ± 0.2^{a}	$(1.0 \pm 0.1) \times 10^{3}$
12	*p*-CN-thioanisole	1.61	$(4.4 \pm 0.2) \times 10^{-2}$	$(6.8 \pm 0.3) \times 10^{-2a}$	$(1.0 \pm 0.1) \times 10^{2}$
			k_{et}, $M^{-1}\ s^{-1}$		
no.	electron donor	E_{ox} (vs SCE, V)[c]	without acid	with $Sc(OTf)_3$ (10 mM)	with HOTf (10 mM)
13	$[Fe^{II}(Ph_2phen)_3]^{2+}$	1.02	NR[d]	$(1.4 \pm 0.1) \times 10^{3a}$	$(7.9 \pm 0.4) \times 10^{3}$
14	$[Fe^{II}(bpy)_3]^{2+}$	1.06	NR[d]	$(2.1 \pm 0.1) \times 10^{2a}$	$(2.5 \pm 0.1) \times 10^{3}$
15	$[Ru^{II}(4,4'\text{-}Me_2bpy)_3]^{2+}$	1.11	NR[d]	$(7.0 \pm 0.3) \times 10$	$(5.0 \pm 0.2) \times 10^{2}$
16	$[Ru^{II}(5,5'\text{-}Me_2bpy)_3]^{2+}$	1.16	NR[d]	$(4.0 \pm 0.2) \times 10$	$(2.5 \pm 0.1) \times 10^{2}$
17	$[Fe^{II}(Clphen)_3]^{2+}$	1.20	NR[d]	9.4 ± 0.4^{a}	$(2.5 \pm 0.1) \times 10^{2}$
18	$[Ru^{II}(bpy)_3]^{2+}$	1.24	NR[d]	9.0 ± 0.4^{a}	$(5.0 \pm 0.2) \times 10$

[a]Taken from ref 23c and 32. [b]Taken from ref 26. [c]Taken from refs 23c 31, and 33. [d]NR = no reaction. [e]The rate constant of the natural decay of $[(N4Py)Fe^{IV}(O)]^{2+}$ in the presence of 10 mM of HOTf in MeCN at 298 K was determined to be 3.0×10^{-6} s^{-1}, which is much smaller than the observed pseudo-first-order rate constants of oxidation of substrates by $[(N4Py)Fe^{IV}(O)]^{2+}$ in the presence of 10 mM of HOTf in MeCN at 298 K.

dx.doi.org/10.1021/ic403124u | Inorg. Chem. 2014, 53, 3618−3628

where k_0, k_1 and k_2 correspond to the rate constants of oxidation of toluene derivatives by $[(N4Py)Fe^{IV}(O)]^{2+}$, the monoprotonated species ($[(N4Py)Fe^{IV}(OH)]^{3+}$) and the diprotonated species ($[(N4Py)Fe^{IV}(OH_2)]^{4+}$), which exhibit zero-, first-, and second-order dependence on [HOTf], respectively.[26] Equation 2 is rewritten by eq 3, which exhibits a linear correlation of $(k_{obs} - k_0)/[HOTf]$ vs [HOTf] as shown in Figure S6 in SI. This indicates that the protonation equilibrium constants were too small to be detected as indicated by no shift of the absorption maximum (695 nm) due to $[(N4Py)Fe^{IV}(O)]^{2+}$ in the presence of 50 mM HOTf (Figure 1). Otherwise, the k_{obs} values in Figure 2 would exhibit a saturation behavior with increasing concentration of HOTf due to the protonation equilibrium.

When HOTf was replaced by $Sc(OTf)_3$, the k_{obs} values of oxidation of toluene derivatives by $[(N4Py)Fe^{IV}(O)]^{2+}$ also increased with increasing concentration of $Sc(OTf)_3$ (Figure S7 in SI). The k_{obs} values of oxidation of toluene derivatives by $[(N4Py)Fe^{IV}(O)]^{2+}$ in the presence of $Sc(OTf)_3$ (10 mM) in MeCN at 298 are also listed in Table 1. The k_{obs} values of oxidation of toluene derivatives (toluene and hexamethylbenzenze) by $[(N4Py)Fe^{IV}(O)]^{2+}$ in the presence of HOTf, $HClO_4$ (70%),[26] and $Sc(OTf)_3$ (50 mM) are compared in Table S1 in SI, where k_{obs} value increases in order: $Sc(OTf)_3$ < $HClO_4$ < HOTf. In the case of hexamethylbenzene, k_{obs} in the presence of HOTf (50 mM) is 2.2×10^5 times larger than that in the absence of HOTf.

When toluene was replaced by the deuterated compound (toluene-d_8), a large deuterium kinetic isotope effect (KIE) was observed in the absence of HOTf (KIE = 31) as shown in Figure 3. Such a large KIE value suggests that the hydrogen

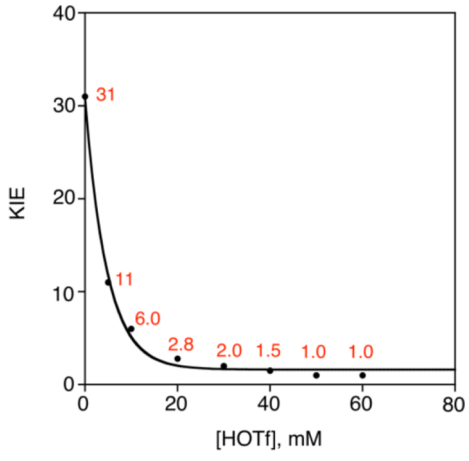

Figure 3. Plot of KIE vs concentration of HOTf in the oxidation of toluene and toluene-d_8 with $[(N4Py)Fe^{IV}(O)]^{2+}$ (0.25 mM) in the presence of HOTf in MeCN at 298 K. Red-colored numbers show the KIE values obtained experimentally.

atom transfer occurs via tunneling in the rate-determining step of oxidation of toluene by $[(N4Py)Fe^{IV}(O)]^{2+}$.[34−37] In the presence of HOTf, the KIE value decreased with increasing concentration of HOTf to reach KIE = 1 at concentrations of HOTf larger than 50 mM (Figure 3). Such a drastic change in KIE from 31 to 1 indicates that the rate-determining step of oxidation of toluene by $[(N4Py)Fe^{IV}(O)]^{2+}$ is changed from hydrogen atom transfer (HAT) in the absence of HOTf to proton-coupled electron transfer (PCET) in the presence of HOTf (> 50 mM).

HOTf- and $Sc(OTf)_3$-Promoted Sulfoxidation of Thioanisole Derivatives by $[(N4Py)Fe^{IV}(O)]^{2+}$. It is well-known that oxidation of thioanisole derivatives by $[(N4Py)Fe^{IV}(O)]^{2+}$ occurs to produce the corresponding sulfoxide products (eq 4).[20a,23c,25]

$$PhSCH_3 + [(N4Py)Fe^{IV}(O)]^{2+} \rightarrow PhS(O)CH_3 + [(N4Py)Fe^{II}]^{2+} \quad (4)$$

The rate of sulfoxidation of thioanisole derivatives by $[(N4Py)Fe^{IV}(O)]^{2+}$ was remarkably enhanced in the presence of $Sc(OTf)_3$ (10 mM) and $HClO_4$ (70%, 10 mM) as compared with that in the absence of acids.[23c,25] The mechanism of sulfoxidation of thioanisole derivatives by $[(N4Py)Fe^{IV}(O)]^{2+}$ is changed from a direct oxygen atom transfer (OAT) pathway to a metal ion-coupled electron transfer (MCET) pathway in the presence of $Sc(OTf)_3$ and also to a PCET pathway in the presence of $HClO_4$.[23c,25] The rate of sulfoxidation of thioanisole derivatives by $[(N4Py)Fe^{IV}(O)]^{2+}$ was further enhanced by the presence of HOTf (10 mM) as compared with that in the presence of $HClO_4$ (70%, 10 mM).[25] The k_{obs} values of oxidation of thioanisole derivatives by $[(N4Py)Fe^{IV}(O)]^{2+}$ in the presence of HOTf (10 mM) were determined from linear plots of k_f vs concentrations of thioanisole derivatives (Figure S8 in SI). The k_{obs} values increase with increasing concentration of HOTf in accordance with eq 2 (Figure S9 in SI).[23c] The k_{obs} values of oxidation of thioanisole derivatives by $[(N4Py)Fe^{IV}(O)]^{2+}$ in the presence of HOTf (10 mM) in MeCN at 298 K are also listed in Table 1.

Inverse Kinetic Isotope Effect in Proton-Coupled Electron Transfer Reduction of $[(N4Py)Fe^{IV}(O)]^{2+}$. When HOTf was replaced by the deuterated acid (DOTf), the k_{et} value of PCET from an electron donor ($[Ru^{II}(bpy)_3]^{2+}$; bpy = 2,2′-bipyridine) to $[(N4Py)Fe^{IV}(O)]^{2+}$ with DOTf in MeCN at 298 K was larger than that with the same concentration of HOTf as shown in Figure 4. Both the k_{et} values with DOTf and HOTf increased with increasing concentration of DOTf and HOTf, respectively, in accordance with eq 2. The KIE value $(k_{obs(HOTf)}/k_{obs(DOTf)})$ was determined to be 0.25 ± 0.05 at HOTf (DOTf) = 2.5 mM, increasing to be a constant value of 0.40 ± 0.04 at the higher concentrations of HOTf (DOTf) as

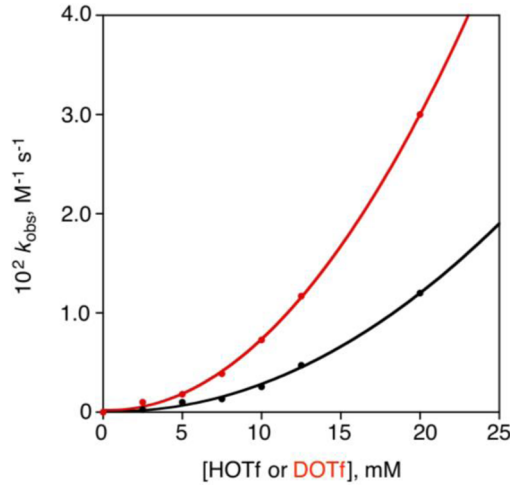

Figure 4. Plots of k_{et} vs [HOTf] (black circles) and [DOTf] (red circles) for PCET from $[Ru^{II}(bpy)_3]^{2+}$ to $[(N4Py)Fe^{IV}(O)]^{2+}$ in the presence of HOTf and DOTf in MeCN at 298 K, respectively.

dx.doi.org/10.1021/ic403124u | Inorg. Chem. 2014, 53, 3618−3628

shown in Figure S10a in SI. Such an inverse KIE indicates that binding of protons to the oxo group to produce the O−H (or O−D) bond is involved in the rate-determining step of PCET from $[Ru^{II}(bpy)_3]^{2+}$ to $[(N4Py)Fe^{IV}(O)]^{2+}$, because an inverse KIE results from a larger zero-point energy difference between the O−H and O−D bonds in the transition state relative to the ground state.[38] Thus, the O−H bonds in the reduced species ($[(N4Py)Fe^{III}(OH)]^{2+}$ and $[(N4Py)Fe^{III}(OH_2)]^{3+}$) are much stronger than those in $[(N4Py)Fe^{IV}(OH)]^{3+}$ and $[(N4Py)Fe^{IV}(OH_2)]^{4+}$, respectively. The larger the difference is in the O−H bond strength between the reduced and oxidized species, the larger may be the inverse KIE. Thus, the larger inverse KIE value at the lower concentration of HOTf suggests that the difference in O−H bond strength between $[(N4Py)Fe^{III}(OH)]^{2+}$ and $[(N4Py)Fe^{IV}(OH)]^{3+}$ (monoprotonated species) may be larger than that between $[(N4Py)Fe^{III}(OH_2)]^{3+}$ and $[(N4Py)Fe^{IV}(OH_2)]^{4+}$ (diprotonated).

A similar inverse KIE was observed for the k_{obs} values of oxidation of toluene by $[(N4Py)Fe^{IV}(O)]^{2+}$ in the presence of large concentrations of DOTf (>50 mM) in comparison with those in the presence of HOTf as shown in Figure 5. The KIE

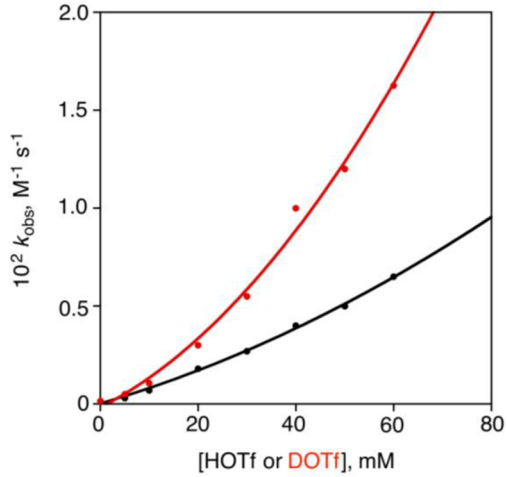

Figure 5. Plots of k_{obs} vs [HOTf] (black circles) and [DOTf] (red circles) for oxidation of toluene by $[(N4Py)Fe^{IV}(O)]^{2+}$ in the presence of HOTf and DOTf in MeCN at 298 K, respectively.

value decreases with increasing concentration of HOTf (Figure S10b in SI) to reach a constant value of 0.42 ± 0.04, which agrees with the KIE value of PCET from $[Ru^{II}(bpy)_3]^{2+}$ to $[(N4Py)Fe^{IV}(O)]^{2+}$ (0.40 ± 0.04) in Figure S10a in SI. The same inverse KIE of the oxidation of toluene as that of PCET together with the absence of KIE between toluene-d_8 and toluene (Figure 3) strongly indicates that the oxidation of toluene by $[(N4Py)Fe^{IV}(O)]^{2+}$ in the presence of large concentrations of HOTf occurs via PCET as the rate-determining step.[39,40]

Comparison of Proton-Coupled Electron Transfer vs Metal Ion-Coupled Electron Transfer. Rates of electron transfer from electron donors to $[(N4Py)Fe^{IV}(O)]^{2+}$ are accelerated by binding of protons and metal ions to $[(N4Py)Fe^{IV}(O)]^{2+}$ via PCET and MCET, respectively.[23b] In order to compare the acceleration effect of HOTf with that of metal triflates ($M^{n+}(OTf)_n$), we determined that rate constant of PCET from ferrocene (Fc) to $[(N4Py)Fe^{IV}(O)]^{2+}$ in the presence of HOTf in MeCN at 298 K. The observed second-order rate constant (k_{et}) of PCET from Fc to $[(N4Py)Fe^{IV}(O)]^{2+}$ increased with increasing concentration of HOTf in accordance with eq 2 as shown in Figure 6 (red line). The

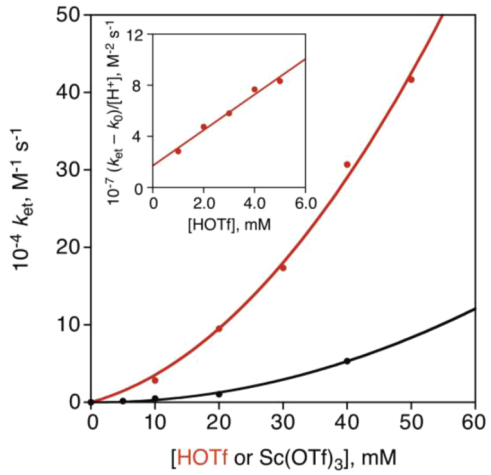

Figure 6. Plots of k_{et} vs [HOTf] (red circles) and [$Sc(OTf)_3$] (black circles) for PCET and MCET from Fc to $[Fe^{IV}(O)(N4Py)]^{2+}$ in the presence of HOTf and $Sc(OTf)_3$ in MeCN at 298 K, respectively. Inset shows plot of $(k_{et} - k_0)/[HOTf]$ vs [HOTf].

linear plot of $(k_{et} - k_0)/[HOTf]$ vs [HOTf] (eq 3) is shown in the inset of Figure 6. The k_1 and k_2 values in eq 3 were determined from the intercept and the slope, respectively.

Similarly, we determined the k_1 and k_2 values of MCET from Fc to $[(N4Py)Fe^{IV}(O)]^{2+}$ in the presence of $Sc(OTf)_3$ in MeCN at 298 K. The dependence of k_{et} on [$Sc(OTf)_3$] is shown in Figure 6 (black line).[23a] The k_{et} values with HOTf are always larger than those with $Sc(OTf)_3$ at the same concentrations of acids. The k_1 and k_2 values with various metal triflates were determined previously from the intercepts and slopes of plots of $(k_{et} - k_0)/[M^{n+}(OTf)_n]$ vs $[M^{n+}(OTf)_n]$, respectively.[23a]

Figure 7 shows plots of log k_1 and log k_2 vs a quantitative measure of Lewis acidity ($\Delta h\nu$) for both PCET and MCET from Fc to $[(N4Py)Fe^{IV}(O)]^{2+}$ in the presence of HOTf and $M^{n+}(OTf)_n$, respectively. The $\Delta h\nu$ values were obtained from the red shifts of the fluorescence emission energies of 10-methylacridone ($\Delta h\nu$) due to binding of metal triflates to the carbonyl oxygen from that in the absence of acids.[41] According to the shift of fluorescence emission energy ($\Delta h\nu$), the relative Lewis acidity of the proton was determined to be 0.26 eV, which is slightly higher than that of $Sc(OTf)_3$ (0.25 eV) as shown in Figure S11 in SI.[41] Good linear correlations were obtained for plots of both log k_1 and log k_2 of PCET and MCET from Fc to $[(N4Py)Fe^{IV}(O)]^{2+}$ vs $\Delta h\nu$ (Figure 7). The stronger the acidity of Lewis acids is, the stronger becomes the binding of acids to $[(N4Py)Fe^{IV}(O)]^{2+}$ as well as to the excited state of AcrCO, resulting in the acceleration of PCET and MCET from Fc to $[(N4Py)Fe^{IV}(O)]^{2+}$.

One Electron Reduction Potentials of $[(N4Py)Fe^{IV}(O)]^{2+}$ in the Presence of HOTf. In order to examine the driving force dependence of PCET from electron donors to $[(N4Py)Fe^{IV}(O)]^{2+}$ in the presence of HOTf in MeCN, the one-electron reduction potentials of $[(N4Py)Fe^{IV}(O)]^{2+}$ in the presence of various concentrations of HOTf were determined by the redox titration (vide infra). When $[Ru^{II}(NO_2phen)_3]^{2+}$ (NO_2phen = 5-nitrophenathrene) was employed as an electron donor, no electron transfer from $[Ru^{II}(NO_2phen)_3]^{2+}$ (E_{ox} =

dx.doi.org/10.1021/ic403124u | Inorg. Chem. 2014, 53, 3618−3628

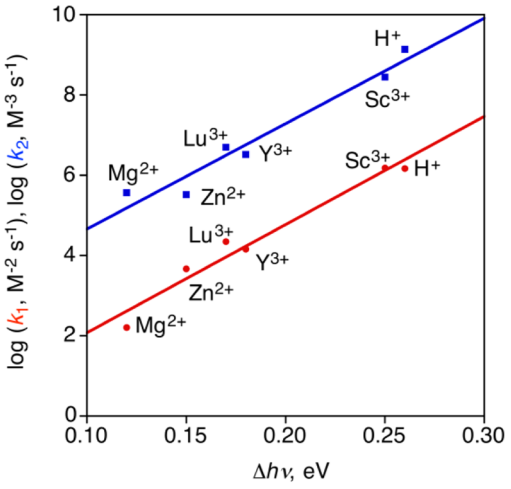

Figure 7. Plots of log k_1 (red circles) and log k_2 (blue squares) vs $\Delta h\nu$ for PCET and MCET from Fc to $[(N4Py)Fe^{IV}(O)]^{2+}$ in the presence of HOTf and metal triflates in MeCN at 298 K, respectively. The $\Delta h\nu$ values were determined from the fluorescence emission energies of AcrCO in the presence of HOTf and metal triflates relative to the energy in their absence.

1.45 V vs SCE, Figure S12 in SI) to $[(N4Py)Fe^{IV}(O)]^{2+}$ (E_{red} = 0.51 V vs SCE)[42] occurred in the absence of acids in MeCN, because the free energy change of electron transfer is highly positive (ΔG_{et} = 0.94 eV), i.e., endergonic. However, the electron transfer occurred efficiently in the presence of HOTf (10 mM) as shown in Figure 8, where the absorption band at

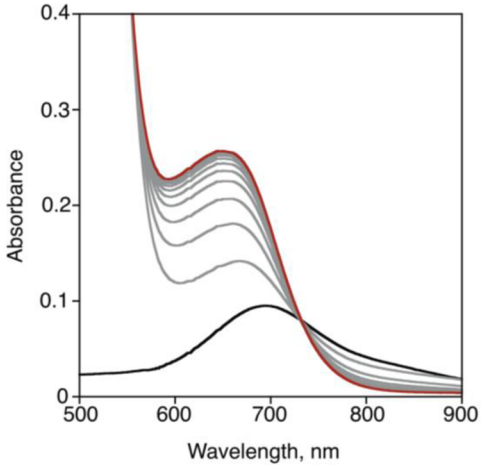

Figure 8. Visible spectral changes observed in PCET from $[Ru^{II}(NO_2phen)_3]^{2+}$ (2.5 mM) to $[(N4Py)Fe^{IV}(O)]^{2+}$ (0.25 mM) in the presence of HOTf (10 mM) in MeCN at 298 K.

695 nm due to $[(N4Py)Fe^{IV}(O)]^{2+}$ (λ_{max} = 695 nm) disappeared, accompanied by the appearance of a new absorption band at 650 nm due to $[Ru^{III}(NO_2phen)_3]^{3+}$ (λ_{max} = 650 nm) with an isosbestic point at 730 nm. The concentration of $[Ru^{III}(NO_2phen)_3]^{3+}$ produced in PCET from $[Ru^{II}(NO_2phen)_3]^{2+}$ to $[(N4Py)Fe^{IV}(O)]^{2+}$ in the presence of HOTf (10 mM) is plotted against the initial concentration of $[Ru^{II}(NO_2phen)_3]^{2+}$ as shown in Figure 9, which indicates that there is a PCET equilibrium as given in eq 5.

$$[(N4Py)Fe^{IV}(O)]^{2+} + [Ru^{II}(NO_2phen)_3]^{2+} + 2H^+ \overset{k_{et}}{\rightleftarrows} [(N4Py)Fe^{III}(OH_2)]^{3+} + [Ru^{III}(NO_2phen)_3]^{3+} \quad (5)$$

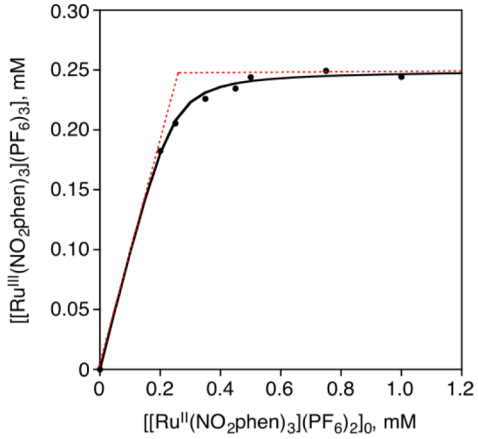

Figure 9. Plot of concentration of $[Ru^{III}(NO_2phen)_3]^{3+}$ produced in PCET from $[Ru^{II}(NO_2phen)_3]^{2+}$ to $[(N4Py)Fe^{IV}(O)]^{2+}$ (0.25 mM) in the presence of HOTf (10 mM) in deaerated MeCN at 298 K vs initial concentration of $[Ru^{II}(NO_2phen)_3](PF_6)_2$, $[Ru^{II}(NO_2phen)_3](PF_6)_2]_0$.

The PCET equilibrium constant K_{et} was determined by fitting the plot in Figure 9 to be K_{et} = 24. The E_{red} value of $[(N4Py)Fe^{IV}(O)]^{2+}$ in the presence of HOTf (10 mM) MeCN at 298 K was determined from the K_{et} value (24) and the E_{ox} value of $[Ru^{II}(NO_2phen)_3]^{2+}$ (E_{ox} = 1.45 V vs SCE) using an Nernst equation (eq 6, where R is the gas constant, T is absolute temperature, and F is the Faraday constant) to be 1.55 V vs SCE,

$$E_{red} = E_{ox} + (RT/F) \ln K_{et} \quad (6)$$

which is much higher than that in the presence of $Sc(OTf)_3$ (10 mM; 1.19 V vs SCE) reported previously.[23b,43] The E_{red} values in the presence of various concentrations of HOTf and $Sc(OTf)_3$ were also determined from the K_{et} values and the E_{ox} value of $[Ru^{II}(NO_2phen)_3]^{2+}$ using eq 6.

The dependence of E_{red} of $[(N4Py)Fe^{IV}(O)]^{2+}$ on log[HOTf] and log[$Sc(OTf)_3$] is shown in Figure 10, where the slopes are determined to be 113 ± 6 mV for HOTf and 118 ± 8 mV for $Sc(OTf)_3$. The Nernst equation for the dependence of E_{red} on log[Acid] (Acid = HOTf and $Sc(OTf)_3$) is given by eq 7, where K_{red1} and K_{red2} are the equilibrium constants for the first and second binding of acids to $[(N4Py)Fe^{III}(O)]^+$, respectively. Under the conditions such that K_{red2}[Acid] ≫ 1, eq 7 is rewritten by eq 8,

$$E_{red} = E^0_{red} + (2.3RT/F) \log(K_{red1}[Acid] + K_{red1}K_{red2}[Acid]^2) \quad (7)$$

$$E_{red} = E^\circ_{red} + 2(2.3RT/F) \log(K_{red1}K_{red2}[Acid]) \quad (8)$$

where the slope of the plot of E_{red} vs log[Acid] is $2(2.3RT/F)$ = 118 mV at 298 K, which agrees well with the experimental values in Figure 10. Such agreement indicates that PCET and MCET reduction of $[(N4Py)Fe^{IV}(O)]^{2+}$ involve binding of two acid molecules of HOTf and $Sc(OTf)_3$ to $[(N4Py)Fe^{III}(O)]^+$, respectively. The second-order rate constants (k_{et}) of electron

dx.doi.org/10.1021/ic403124u | Inorg. Chem. 2014, 53, 3618−3628

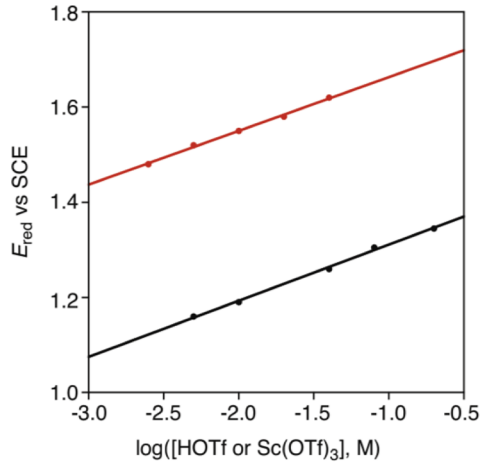

Figure 10. Dependence of E_{red} of $[(N4Py)Fe^{IV}(O)]^{2+}$ on log[HOTf] (red circles) and log[$Sc(OTf)_3$] (black circles) in deaerated MeCN at 298. Black and red lines are fitted by eq 8.

transfer from electron donors to $[(N4Py)Fe^{IV}(O)]^{2+}$ in the presence of HOTf (10 mM) and $Sc(OTf)_3$ (10 mM) were determined as listed in Table 1 (Figures S13 and S14 in SI).

Unified Driving Force Dependence of Rate Constants. The dependence of log k_{obs} of oxidation of toluene and thioanisole derivatives by $[(N4Py)Fe^{IV}(O)]^{2+}$ in the presence of HOTf (10 mM) and $Sc(OTf)_3$ (10 mM) on one-electron oxidation potentials (E_{ox}) of electron donors including toluene and thioanisole derivatives is shown in Figure 11 (red line). A

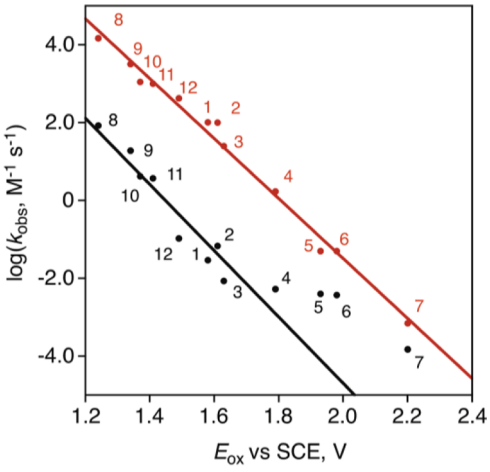

Figure 11. Plot of log k_{obs} vs oxidation potentials (E_{ox}) of toluene and thioanisole derivatives [(1) hexamethylbenzene, (2) 1,2,3,4,5-pentamethylbenzene, (3) 1,2,4,5-tetramethylbenzene, (4) 1,2,4-trimethylbenzene, (5) 1,4-dimethylbenzene, (6) 1,3,5-trimethylbenzene, (7) toluene, (8) *p*-Me-thioanisole, (9) thioanisole, (10) *p*-Cl-thioanisole, (11) *p*-Br-thioanisole, and (12) *p*-CN-thioanisole] in the C−H bond cleavage of toluene derivatives and sulfoxidation of thioanisole derivatives by $[(N4Py)Fe^{IV}(O)]^{2+}$ in the presence of 10 mM of HOTf (red circles) and $Sc(OTf)_3$ (black circles) in MeCN at 298 K.

unified correlation is observed for plots of log k_{obs} of oxidation of toluene and thioanisole derivatives by $[(N4Py)Fe^{IV}(O)]^{2+}$ in the presence of HOTf (10 mM) vs the E_{ox} values of toluene and thioanisole derivatives. Such a unified correlation suggests that oxidation of both toluene and thioanisole derivatives by $[(N4Py)Fe^{IV}(O)]^{2+}$ in the presence of HOTf (10 mM) proceeds via PCET from toluene and thioanisole derivatives to $[(N4Py)Fe^{IV}(O)]^{2+}$ and the reorganization energies of the electron donors are virtually the same as reported for photoinduced electron-transfer reactions of aromatic compounds.[32] However, the log k_{et} values of PCET from coordinatively saturated metal complexes (nos. 13−18 in Table 1) to $[(N4Py)Fe^{IV}(O)]^{2+}$ are significantly smaller than log k_{obs} values of oxidation of toluene and thioanisole derivatives (red line in Figure 11).

Similarly a unified linear correlation is observed for plots of log k_{obs} of oxidation of toluene and thioanisole derivatives by $[(N4Py)Fe^{IV}(O)]^{2+}$ in the presence of $Sc(OTf)_3$ (10 mM) vs the E_{ox} values of toluene and thioanisole derivatives when the E_{ox} values are lower than 1.6 V vs SCE (black line in Figure 11). Such a unified correlation indicates that oxidation of toluene and thioanisole derivatives by $[(N4Py)Fe^{IV}(O)]^{2+}$ in the presence of $Sc(OTf)_3$ (10 mM) proceeds via MCET from toluene and thioanisole derivatives to $[(N4Py)Fe^{IV}(O)]^{2+}$. In the case of 1,2,4-trimethylbenzene (No. 4), 1,4-dimethylbenzene (No. 5), 1,3,5-trimethylbenzene (No. 6) and toluene (No. 7), which have higher E_{ox} values than 1.6 V vs SCE, however, the log k_{obs} values are significantly larger than the linear correlation (black line in Figure 11). The log k_{et} values of MCET from coordinatively saturated metal complexes (Nos. 13−18 in Table 1) to $[(N4Py)Fe^{IV}(O)]^{2+}$ are also significantly smaller than the log k_{obs} values of oxidation of toluene and thioanisole derivatives (black line in Figure 11).

The difference in log k_{et} and log k_{obs} values between PCET and MCET is expected to result from the difference in the E_{red} values of $[(N4Py)Fe^{IV}(O)]^{2+}$ in the presence of HOTf (10 mM) and $Sc(OTf)_3$ (10 mM). Driving forces of the PCET and MCET reactions ($-\Delta G_{et}$ in eV) are obtained from the one-electron oxidation potentials (E_{ox}) of electron donors (coordinatively saturated metal complexes, toluene and thioanisole derivatives) and the one-electron reduction potentials (E_{red}) of $[(N4Py)Fe^{IV}(O)]^{2+}$ in the presence of acids as given by eq 9, where e is the elementary charge.

$$-\Delta G_{et} = e(E_{red} - E_{ox}) \quad (9)$$

The driving force dependence of log k_{et} of electron transfer from coordinatively saturated metal complexes to $[(N4Py)Fe^{IV}(O)]^{2+}$ in the absence and presence of 10 mM of HOTf (black line in Figure 12) is well fitted by the Marcus equation of outer-sphere electron transfer (eq 10),[44]

$$k_{et} = Z \exp[-(\lambda/4)(1 + \Delta G_{et}/\lambda)^2/k_B T] \quad (10)$$

where Z is the frequency factor, which is $k_B TK/h$ (k_B is the Boltzmann constant, T is absolute temperature, K is the formation constant of the precursor complex and h is the Planck constant), using the same value of reorganization energy of electron transfer (λ = 2.74 eV).

The Z value of outer-sphere electron-transfer reactions is normally taken as 1.0×10^{11} M^{-1} s^{-1}.[45−48] This indicates that the K value of outer-sphere electron-transfer reactions is as small as 0.020 M^{-1}, because there is little interaction in the precursor complex for outer-sphere electron-transfer reactions of coordinatively saturated metal complexes.

The log k_{obs} values of oxidation of toluene and thioanisole derivatives by $[(N4Py)Fe^{IV}(O)]^{2+}$ in the presence of HOTf and $Sc(OTf)_3$ (10 mM) as well as the log k_{et} values of MCET from coordinatively saturated metal complexes to $[(N4Py)Fe^{IV}(O)]^{2+}$ in the presence of $Sc(OTf)_3$ (10 mM) are larger than those expected by eq 10 with λ = 2.74 eV. The log k_{obs} values of oxidation of toluene and thioanisole derivatives by

dx.doi.org/10.1021/ic403124u | Inorg. Chem. 2014, 53, 3618−3628

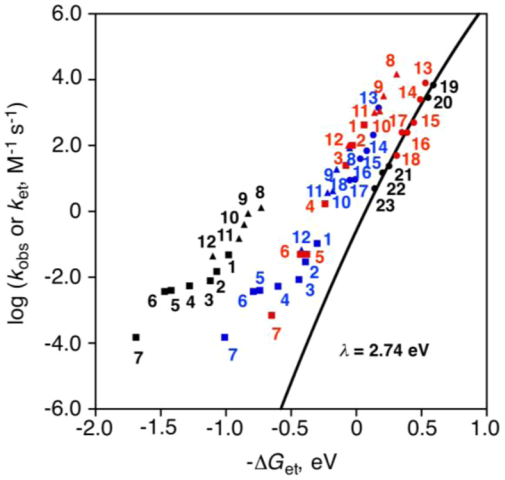

Figure 12. Plots of log k_{obs} for oxidation of toluene and thioanisole derivatives [(1) hexamethylbenzene, (2) 1,2,3,4,5-pentamethylbenzene, (3) 1,2,4,5-tetramethylbenzene, (4) 1,2,4-trimethylbenzene, (5) 1,4-dimethylbenzene, (6) 1,3,5-trimethylbenzene, (7) toluene, (8) *p*-Me-thioanisole, (9) thioanisole, (10) *p*-Cl-thioanisole, (11) *p*-Br-thioanisole, and (12) *p*-CN-thioanisole] by $[(N4Py)Fe^{IV}(O)]^{2+}$ in the absence (black) and presence of 10 mM of HOTF (red) and $Sc(OTf)_3$ (blue) in MeCN at 298 K vs the driving force of electron transfer $[-\Delta G = e(E_{red} - E_{ox})]$ from toluene derivatives (squares) and thioanisole derivatives (triangles) to $[(N4Py)Fe^{IV}(O)]^{2+}$ in the presence of HOTf (red) and $Sc(OTf)_3$ (blue). The red and blue circles show the driving force dependence of the rate constants (log k_{et}) of electron transfer from electron donors [(13) $[Fe^{II}(Ph_2phen)_3]^{2+}$, (14) $[Fe^{II}(bpy)_3]^{2+}$, (15) $[Ru^{II}(4,4'\text{-}Me_2phen)_3]^{2+}$, (16) $[Ru^{II}(5,5'\text{-}Me_2phen)_3]^{2+}$, (17) $[Fe^{II}(Clphen)_3]^{2+}$, and (18) $[Ru^{II}(bpy)_3]^{2+}$] to $[(N4Py)Fe^{IV}(O)]^{2+}$ in the presence of HOTf (10 mM) and $Sc(OTf)_3$ (10 mM) in MeCN at 298 K. The black line is drawn using eq 10 with λ = 2.74 eV.[25,42] The black circles show the driving force dependence of the rate constants (log k_{et}) of electron transfer from electron donors [(19) decamethylferrocene, (20) octamethylferrocene, (21) 1.1′-dimethylferrocene, (22) *n*-amylferrocene, and (23) ferrocene] to $[(N4Py)Fe^{IV}(O)]^{2+}$ in the absence of acids in MeCN at 298 K.[42]

$[(N4Py)Fe^{IV}(O)]^{2+}$ in the presence of HOTf and $Sc(OTf)_3$ larger than the log k_{et} values of electron transfer from coordinatively saturated metal complexes to $[(N4Py)Fe^{IV}(O)]^{2+}$ in the presence of HOTf may result from the difference in the *K* values of precursor complexes, because the stronger interaction of $[(N4Py)Fe^{IV}(OH_2)]^{4+}$ with toluene and thioanisole derivatives is expected as compared with that with coordinatively saturated metal complexes. This was confirmed by examining the dependence of the pseudo-first-order rate constants (k_f) on concentrations of toluene and thioanisole derivatives in the large concentration range (vide infra). The k_f values of oxidation of *p*-CN-thioanisole by $[(N4Py)Fe^{IV}(O)]^{2+}$ in the presence of HOTf (10 mM) and $Sc(OTf)_3$ (10 mM) are shown respectively in a and b of Figure 13. In both cases, the k_f values increase with increasing concentration of *p*-CN-thioanisole to approach constant values. Such a saturation behavior indicates formation of the precursor complex prior to electron transfer when k_f is given by eq 11, where k_{ET} is the first-order rate constant of electron transfer in the precursor complex, *K* is the formation constant of the precursor complex, and [S] is concentration of a substrate. Equation 11 is rewritten by eq 12, which predicts a linear correlation between k_f^{-1} and $[S]^{-1}$.

$$k_f = k_{ET}K[S]/(1 + K[S]) \quad (11)$$

$$k_f^{-1} = (k_{ET}K[S])^{-1} + k_{ET}^{-1} \quad (12)$$

From the intercepts and slopes of linear plots of k_f^{-1} and $[S]^{-1}$ (Figure S15 in SI), the *K* values were determined as listed in Table 2. The *K* values of oxidation of 1,2,4,5-tetramethylbenzene and 1,2,4-trimethylbenzene by $[(N4Py)Fe^{IV}(O)]^{2+}$ in the presence of HOTf (10 mM) and $Sc(OTf)_3$ (10 mM) were also determined as listed in Table 2 (Figures S16–S18 in SI).

Table 2. Formation Constants of Precursor Complexes in Oxidation of Toluene and Thioanisole Derivatives by $[(N4Py)Fe^{IV}(O)]^{2+}$ in the Presence of Acids (10 mM), HOTf and $Sc(OTf)_3$, in MeCN at 298 K

toluene and thioanisole derivative	formation constant (*K*, M^{-1})	
	10 mM of $Sc(OTf)_3$	10 mM of HOTf
1,2,4,5-tetramethylbenzene	3.0 ± 0.2	(1.2 ± 0.4) × 10^2
1,2,4-trimethylbenzene	2.5 ± 0.1	(1.0 ± 0.1) × 10^2
p-Cl-thioanisole	3.1 ± 0.2	(9.6 ± 0.5) × 10
p-CN-thioanisole	2.7 ± 0.2	(4.0 ± 0.5) × 10

The *K* value of the precursor complexes of $[(N4Py)Fe^{IV}(O)]^{2+}$ with 1,2,4,5-tetramethylbenzene in the presence of 10 mM HOTf (K = 120 M^{-1}) is much larger than that of $[(N4Py)Fe^{IV}(O)]^{2+}$ with the same substrate in the presence of 10 mM $Sc(OTf)_3$ (K = 3.0 M^{-1}). The same trend is observed

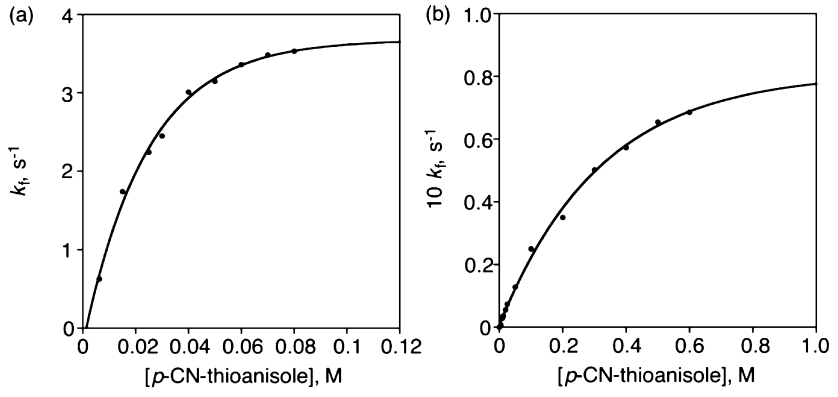

Figure 13. Plots of pseudo-first-order rate constants (k_f) of oxidation of *p*-CN-thioanisole by $[(N4Py)Fe^{IV}(O)]^{2+}$ (0.25 mM) in the presence of (a) HOTf (10 mM) and (b) $Sc(OTf)_3$ (10 mM) in MeCN at 298 K vs concentration of *p*-CN-thioanisole.

dx.doi.org/10.1021/ic403124u | *Inorg. Chem.* 2014, 53, 3618–3628

for other substrates as listed in Table 2. The significantly smaller K values with $Sc(OTf)_3$ (10 mM) than those with HOTf (10 mM) may be ascribed to the large steric effect of two molecules of $Sc(OTf)_3$ bound to $[(N4Py)Fe^{IV}(O)]^{2+}$ as compared with that of HOTf. In each case, the K values are significantly larger than those employed for outer-sphere electron-transfer reactions of coordinatively saturated metal complexes (K = ~0.020 M^{-1}).

Although K values may be changed depending on the E_{ox} values of toluene and thioanisole derivatives, the k_{ET} values were evaluated by using averaged K values with HOTf [(9 ± 2) × 10 M^{-1}] and $Sc(OTf)_3$ (2.8 ± 0.2 M^{-1}) in Table 2. Figure 14

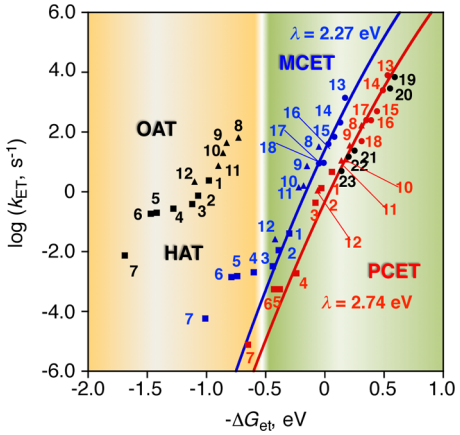

Figure 14. Plots of log k_{ET} for C–H bond cleavage of toluene derivatives and sulfoxidation of thioanisole derivatives [(1) hexamethylbenzene, (2) 1,2,3,4,5-pentamethylbenzene, (3) 1,2,4,5-tetramethylbenzene, (4) 1,2,4-trimethylbenzene, (5) 1,4-dimethylbenzene, (6) 1,3,5-trimethylbenzene, (7) toluene, (8) *p*-Me-thioanisole, (9) thioanisole, (10) *p*-Cl-thioanisole, (11) *p*-Br-thioanisole and (12) *p*-CN-thioanisole] by $[(N4Py)Fe^{IV}(O)]^{2+}$ in the absence (black) and presence of acids (10 mM), HOTf (red) and $Sc(OTf)_3$ (blue), in MeCN at 298 K vs the driving force of electron transfer [$-\Delta G = e(E_{red} - E_{ox})$] from toluene derivatives (squares) and thioanisole derivatives (triangles) to $[(N4Py)Fe^{IV}(O)]^{2+}$ in the presence of HOTf (red) and $Sc(OTf)_3$ (blue). The red and blue circles show the driving force dependence of the rate constants (log k_{et}) of electron transfer from electron donors [(13) $[Fe^{II}(Ph_2phen)_3]^{2+}$, (14) $[Fe^{II}(bpy)_3]^{2+}$, (15) $[Ru^{II}(4,4'\text{-}Me_2phen)_3]^{2+}$, (16) $[Ru^{II}(5,5'\text{-}Me_2phen)_3]^{2+}$, (17) $[Fe^{II}(Clphen)_3]^{2+}$ and (18) $[Ru^{II}(bpy)_3]^{2+}$] to $[(N4Py)Fe^{IV}(O)]^{2+}$ in the presence of acids (10 mM), HOTf and $Sc(OTf)_3$, in MeCN at 298 K, respectively. The black circles show the driving force dependence of the rate constants (log k_{et}) of electron transfer from electron donors [(19) decamethylferrocene, (20) octamethylferrocene, (21) 1.1′-dimethylferrocene, (22) *n*-amylferrocene and (23) ferrocene] to $[(N4Py)Fe^{IV}(O)]^{2+}$ in the absence of acids in MeCN at 298 K.[42]

shows unified plots of log k_{ET} of PCET and MCET from electron donors to $[(N4Py)Fe^{IV}(O)]^{2+}$ in the presence of HOTf (10 mM) and $Sc(OTf)_3$ (10 mM). The driving force dependence of log k_{ET} (or log k_{obs}) of PCET from all kinds of electron donors (coordinatively saturated metal complexes, toluene and thioanisole derivatives) to $[(N4Py)Fe^{IV}(O)]^{2+}$ in the presence of HOTf (10 mM) in MeCN at 298 K is unified as a red line together with that of log k_{ET} of electron transfer from coordinatively saturated metal complexes to $[(N4Py)Fe^{IV}(O)]^{2+}$ in the absence of HOTf using the same λ value of 2.74 eV.[42] The driving force dependence of log k_{ET} of MCET from all kinds of electron donors to $[(N4Py)Fe^{IV}(O)]^{2+}$ in the presence of $Sc(OTf)_3$ (10 mM) in MeCN at 298 K is also unified as a blue line using the same λ value of 2.27 eV. When the driving forces of MCET ($Sc(OTf)_3$) and PCET (HOTf) are more negative than −0.5 eV, the k_{ET} values become larger than those predicted by the Marcus lines (Figure 14). The λ value of the MCET (2.27 eV) smaller than that of the PCET (2.74 eV) may be ascribed to the smaller change in the Fe–O distance associated with the MCET than that with the PCET at the same concentration of acids probably due to the steric effect of two molecules of $Sc(OTf)_3$ bound to the oxo group.

The unified correlations of driving force dependence of log k_{ET} of PCET and MCET from all kinds of electron donors to $[(N4Py)Fe^{IV}(O)]^{2+}$ in Figure 14 indicate that oxidation of toluene and thioanisole derivatives by $[(N4Py)Fe^{IV}(O)]^{2+}$ in the presence of HOTf and $Sc(OTf)_3$ proceeds via the rate-determining electron transfer from toluene and thioanisole derivatives to $[(N4Py)Fe^{IV}(O)]^{2+}$ which binds with two molecules of $Sc(OTf)_3$ and HOTf, respectively, following formation of the precursor complexes as shown in Scheme 1, provided that the driving force of the electron transfer is larger than −0.5 eV. In the case of oxidation of toluene derivatives by $[(N4Py)Fe^{IV}(O)]^{2+}$ in the presence of HOTf and $Sc(OTf)_3$, the rate-determining PCET and MCET may be followed by rapid proton transfer and the oxygen rebound to produce the corresponding benzyl alcohol derivatives and $[(N4Py)Fe^{II}]^{2+}$, which is oxidized by $[(N4Py)Fe^{IV}(O)]^{2+}$ to $[(N4Py)Fe^{III}]^{3+}$ in the presence of HOTf and $Sc(OTf)_3$. In the case of oxidation of thioanisole derivatives by $[(N4Py)Fe^{IV}(O)]^{2+}$ in the presence of HOTf and $Sc(OTf)_3$, the PCET and MCET may be followed by rapid $O^{\bullet-}$ transfer to produce the corresponding sufoxide derivatives and $[(N4Py)Fe^{II}]^{2+}$, which is also oxidized by $[(N4Py)Fe^{IV}(O)]^{2+}$ to $[(N4Py)Fe^{III}]^{3+}$ in the presence of HOTf and $Sc(OTf)_3$. However, the detailed mechanism after the rate-determining PCET and MCET has yet to be clarified.

In the absence of HOTf and $Sc(OTf)_3$, the k_{ox} values of oxidation of toluene and thioanisole derivatives by $[(N4Py)Fe^{IV}(O)]^{2+}$ are much larger than those predicted from PCET or MCET reactions (black circles in Figure 14). Thus, C–H bond cleavage of toluene derivatives and sulfoxidation of thioanisole derivatives proceed via direct hydrogen atom transfer from toluene derivatives to $[(N4Py)Fe^{IV}(O)]^{2+}$ and oxygen atom transfer from thioanisole derivatives to $[(N4Py)Fe^{IV}(O)]^{2+}$, respectively, rather than an electron-transfer pathway.

CONCLUSION

Oxidation of toluene and thioanisole derivatives by $[(N4Py)Fe^{IV}(O)]^{2+}$ in deaerated MeCN at 298 K was remarkably accelerated by the presence of HOTf and $Sc(OTf)_3$ to yield a stoichiometric amount of the corresponding benzyl alcohol and sulfoxide derivatives, respectively. No KIE was observed when toluene was replaced by toluene-d_8 for the oxidation by $[(N4Py)Fe^{IV}(O)]^{2+}$ in the presence of HOTf (>50 mM), suggesting that the rate-determining step is PCET from toluene to $[(N4Py)Fe^{IV}(O)]^{2+}$. An inverse KIE was observed for PCET from both $[Ru^{II}(bpy)_3]^{2+}$ and toluene to $[(N4Py)Fe^{IV}(O)]^{2+}$ when HOTf was replaced by DOTf, suggesting that the O–H bond of the protonated $Fe^{IV}(O)$ complex at the transition state of PCET is significantly stronger than that of the ground state. The unified correlations of driving force ($-\Delta G_{et}$) dependence of log k_{ET} of oxidation of toluene and thioanisole derivatives by $[(N4Py)Fe^{IV}(O)]^{2+}$ as well as electron transfer from coordinatively saturated metal complexes to $[(N4Py)Fe^{IV}(O)]^{2+}$ in the presence of HOTf and $Sc(OTf)_3$ (Figure 14) indicate that oxidation of toluene and thioanisole

dx.doi.org/10.1021/ic403124u | Inorg. Chem. 2014, 53, 3618–3628

Scheme 1. Proposed Unified Mechanism of Oxidation of Toluene and Thioanisole Derivatives by $[(N4Py)Fe^{IV}(O)]^{2+}$ in the Presence of HOTf and $Sc(OTf)_3$

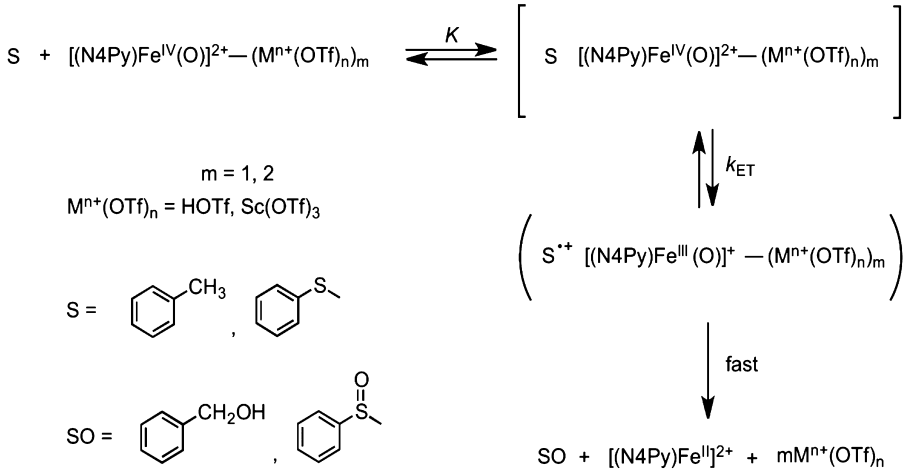

derivatives by $[(N4Py)Fe^{IV}(O)]^{2+}$ in the presence of HOTf and $Sc(OTf)_3$ proceeds via the rate-determining PCET and MCET, respectively. Remarkable enhancement of PCET and MCET reactivity of $[(N4Py)Fe^{IV}(O)]^{2+}$ results from binding of two molecules of HOTf and $Sc(OTf)_3$ to the oxo group of the $Fe^{IV}(O)$ complex, which causes large positive shifts of the E_{red} values in the presence of HOTf and $Sc(OTf)_3$, respectively. Formation of strong precursor complexes of $[(N4Py)Fe^{IV}(O)]^{2+}$, which binds with two molecules of HOTf and $Sc(OTf)_3$, with organic substrates (toluene and thioanisole derivatives) as compared with coordinatively saturated metal complexes also results in enhancement of the PCET and MCET reactivity. A boundary between electron transfer vs concerted pathways is determined by the driving force of electron transfer ($-\Delta G_{et}$). PCET and MCET pathways are dominant when $-\Delta G_{et} > -0.5$ eV, whereas concerted pathways become dominant when $-\Delta G_{et} < -0.5$ eV. The unified view of enhancement of oxidative C−H bond cleavage of toluene derivatives and sulfoxidation of thioanisole derivatives by a nonheme iron(IV)−oxo complex via PCET and MCET demonstrated in this study provides generalized understanding of a variety of PCET and MCET pathways for oxidation of substrates by metal−oxygen species.

■ ASSOCIATED CONTENT

Supporting Information

Table S1 and Figures S1−S18. This material is available free of charge via the Internet at http://pubs.acs.org.

■ AUTHOR INFORMATION

Corresponding Authors

*E-mail: fukuzumi@chem.eng.osaka-u.ac.jp (S.F.)
*E-mail: wwnam@ewha.ac.kr (W.N.)

Notes

The authors declare no competing financial interest.

■ ACKNOWLEDGMENTS

The research at OU was supported by an ALCA funding from Japan Science and Technology Agency (JST), Japan (to S.F.). The research at EWU was supported by NRF/MEST of Korea through CRI (NRF-2012R1A3A2048842 to W.N.) and GRL (NRF-2010-00353 to W.N.). J.P. and Y.M. gratefully acknowledge support from JSPS by a Grant-in-Aid for JSPS fellowship for young scientists.

■ REFERENCES

(1) (a) Ortiz de Montellano, P. R. *Cytochrome P450: Structure, Mechanism, and Biochemistry*, 3rd ed.; Kluwer Academic/Plenum Publishers: New York, 2005. (b) Meunier, B., Ed. *Biomimetic Oxidations Catalyzed by Transition Metal Complexes*; Imperial College Press: London, 2000. (c) *The Ubiquitous Role of Cytochrome P450 Proteins in Metal Ions in Life Sciences*; Sigel, A., Sigel, H., Sigel, R. K. O., Eds.; John Wiley & Sons Ltd.: Chichester, England, 2007; Vol. 3. (d) Grinkova, Y. V.; Denisov, I. G.; McLean, M. A.; Sligar, S. G. *Biol. Biophys. Res. Commun.* **2013**, *430*, 1223.

(2) (a) Sharma, V. K. *Oxidation of Amino Acids, Peptides, and Proteins*; John Wiley & Sons Ltd: Chichester, England, 2012. (b) Sono, M.; Roach, M. P.; Coulter, E. D.; Dawson, J. H. *Chem. Rev.* **1996**, *96*, 2841. (c) Watanabe, Y. *J. Biol. Inorg. Chem.* **2001**, *6*, 846. (d) Jung, C. *Biochim. Biophys. Acta* **2011**, *1814*, 46.

(3) Rohde, J.-U.; In, J.-H.; Lim, M. H.; Brennessel, W. W.; Bukowski, M. R.; Stubna, A.; Münck, E.; Nam, W.; Que, L., Jr. *Science* **2003**, *299*, 1037.

(4) (a) Usharani, D.; Lacy, D. C.; Borovik, A. S.; Shaik, S. *J. Am. Chem. Soc.* **2013**, *135*, 17090. (b) de Visser, S. P.; Rohde, J.-U.; Lee, Y.-M.; Cho, J.; Nam, W. *Coord. Chem. Rev.* **2013**, *257*, 381. (c) McDonald, A. R.; Que, L., Jr. *Coord. Chem. Rev.* **2013**, *257*, 414.

(5) (a) Meunier, B.; de Visser, S. P.; Shaik, S. *Chem. Rev.* **2004**, *104*, 3947. (b) Shaik, S.; Cohen, S.; Wang, Y.; Chen, H.; Kumar, D.; Thiel, W. *Chem. Rev.* **2010**, *110*, 949. (c) Abu-Omar, M. M.; Loaiza, A.; Hontzeas, N. *Chem. Rev.* **2005**, *105*, 2227. (d) Denisov, I. G.; Makris, T. M.; Sligar, S. G.; Schlichting, I. *Chem. Rev.* **2005**, *105*, 2253. (e) Ortiz de Montellano, P. R. *Chem. Rev.* **2010**, *110*, 932.

(6) (a) Bakac, A. *Coord. Chem. Rev.* **2006**, *250*, 2046. (b) Arias, J.; Newlands, C. R.; Abu-Omar, M. M. *Inorg. Chem.* **2001**, *40*, 2185. (c) Sarauli, D.; Meier, R.; Liu, G.-F.; Ivanović-Burmazović, I.; van Eldik, R. *Inorg. Chem.* **2005**, *44*, 7624.

(7) Hayashi, H.; Fujinami, S.; Nagatomo, S.; Ogo, S.; Suzuki, M.; Uehara, A.; Watanabe, Y.; Kitagawa, T. *Inorg. Chim. Acta* **2000**, *300*−*302*, 587.

(8) Das, D.; Sarkar, B.; Kumar Mondal, T.; Mobin, S. M.; Fiedler, J.; Kaim, W.; Kumar Lahiri, G. *Inorg. Chem.* **2011**, *50*, 7090.

(9) (a) Groves, J. T.; Shalyaev, K.; Lee, J. In *The Porphyrin Handbook*; Kadish, K. M., Smith, K. M., Guilard, R., Eds.; Academic Press: Elsevier Science (USA), 2000, Vol. *4*, pp 17−40. (b) Watanabe, Y. In *The Porphyrin Handbook*; Kadish, K. M., Smith, K. M., Guilard, R., Eds.; Academic Press: Elsevier Science (USA), 2000, Vol. *4*, pp 97−117. (c) Groves, J. T. *J. Inorg. Biochem.* **2006**, *100*, 434.

(10) (a) Gunay, A.; Theopold, K. H. *Chem. Rev.* **2010**, *110*, 1060. (b) Che, C.-M.; Lo, V. K.-Y.; Zhou, C.-Y.; Huang, J.-S. *Chem. Soc. Rev.* **2011**, *40*, 1950. (c) Costas, M. *Coord. Chem. Rev.* **2011**, *255*, 2912.
(11) (a) Cho, K.; Leeladee, P.; McGown, A. J.; DeBeer, S.; Goldberg, D. P. *J. Am. Chem. Soc.* **2012**, *134*, 7392. (b) Cho, K.-B.; Chen, H.; Janardanan, D.; de Visser, S. P.; Shaik, S.; Nam, W. *Chem. Commun.* **2012**, *48*, 2189. (c) Seo, M. S.; Kim, N. H.; Cho, K.-B.; So, J. E.; Park, S. K.; Clemancey, M.; Garcia-Serres, R.; Latour, J.-M.; Shaik, S.; Nam, W. *Chem. Sci.* **2011**, *2*, 1039. (d) Borovik, A. S. *Chem. Soc. Rev.* **2011**, *40*, 1870. (e) Janardanan, D.; Wang, Y.; Schyman, P.; Que, L., Jr.; Shaik, S. *Angew. Chem., Int. Ed.* **2010**, *49*, 3342.
(12) (a) Shaik, S.; Chen, H.; Janardanan, D. *Nature Chem.* **2011**, *3*, 19. (b) Chen, H.; Lai, W.; Shaik, S. *J. Phys. Chem. Lett.* **2010**, *1*, 1533.
(13) (a) Krebs, C.; Fujimori, D. G.; Walsh, C. T.; Bollinger, J. M., Jr. *Acc. Chem. Res.* **2007**, *40*, 484. (b) Que, L., Jr. *Acc. Chem. Res.* **2007**, *40*, 493. (c) Nam, W. *Acc. Chem. Res.* **2007**, *40*, 522. (d) Borovik, A. S. *Acc. Chem. Res.* **2005**, *38*, 54. (e) Shaik, S.; Lai, W.; Chen, H.; Wang, Y. *Acc. Chem. Res.* **2010**, *43*, 1154.
(14) Hong, S.; Lee, Y.-M.; Cho, K.-B.; Sundaravel, K.; Cho, J.; Kim, M. J.; Shin, W.; Nam, W. *J. Am. Chem. Soc.* **2011**, *133*, 11876.
(15) Tang, H.; Guan, J.; Zhang, L.; Liu, H.; Huang, X. *Phys. Chem. Chem. Phys.* **2012**, *14*, 12863.
(16) Kumar, D.; Sastry, G. N.; de Visser, S. P. *J. Phys. Chem. B* **2012**, *116*, 718.
(17) (a) Groves, J. T.; McClusky, G. A. *J. Am. Chem. Soc.* **1976**, *98*, 859. (b) Ortiz de Montellano, P. R.; Stearns, R. A. *J. Am. Chem. Soc.* **1987**, *109*, 3415. (c) Schöoneboom, J. C.; Cohen, S.; Lin, H.; Shaik, S.; Thiel, W. *J. Am. Chem. Soc.* **2004**, *126*, 4017. (d) Hirao, H.; Kumar, D.; Que, L., Jr.; Shaik, S. *J. Am. Chem. Soc.* **2006**, *128*, 8590.
(18) Chiavarino, B.; Cipollini, R.; Crestoni, M. E.; Fornarini, S.; Fornarini, S.; Lapi, A. *J. Am. Chem. Soc.* **2008**, *130*, 3208.
(19) Kaizer, J.; Klinker, E. J.; Oh, N. Y.; Rohde, J.-U.; Song, W. J.; Stubna, A.; Kim, J.; Münck, E.; Nam, W.; Que, L., Jr. *J. Am. Chem. Soc.* **2004**, *126*, 472.
(20) (a) Park, M. J.; Lee, J.; Suh, Y.; Kim, J.; Nam, W. *J. Am. Chem. Soc.* **2006**, *128*, 2630. (b) Sastri, C. V.; Lee, J.; Oh, K.; Lee, Y. J.; Lee, J.; Jackson, T. A.; Ray, K.; Hirao, H.; Shin, W.; Halfen, J. A.; Kim, J.; Que, L., Jr.; Shaik, S.; Nam, W. *Proc. Natl. Acad. Sci. U.S.A.* **2007**, *104*, 19181. (c) Jeong, Y. J.; Kang, Y.; Han, A.-R.; Lee, Y.-M.; Kotani, H.; Fukuzumi, S.; Nam, W. *Angew. Chem., Int. Ed.* **2008**, *47*, 7321. (d) Lee, Y.-M.; Dhuri, S. N.; Sawant, S. C.; Cho, J.; Kubo, M.; Ogura, T.; Fukuzumi, S.; Nam, W. *Angew. Chem., Int. Ed.* **2009**, *48*, 1803.
(21) (a) Lee, Y.-M.; Hong, S.; Morimoto, Y.; Shin, W.; Fukuzumi, S.; Nam, W. *J. Am. Chem. Soc.* **2010**, *132*, 10668. (b) Wilson, S. A.; Chen, J.; Hong, S.; Lee, Y.-M.; Clémancey, M.; Garcia-Serres, R.; Nomura, T.; Ogura, T.; Latour, J.-M.; Hedman, B.; Hodfson, K. O.; Nam, W.; Solomon, E. I. *J. Am. Chem. Soc.* **2012**, *134*, 11791.
(22) (a) Yiu, S.-M.; Man, W.-L.; Lau, T.-C. *J. Am. Chem. Soc.* **2008**, *130*, 10821. (b) Lam, W. W. Y.; Yiu, S.-M.; Lee, J. M. N.; Yau, S. K. Y.; Kwong, H.-K.; Lau, T.-C.; Liu, D.; Lin, Z. *J. Am. Chem. Soc.* **2006**, *128*, 2851. (c) Yiu, S.-M.; Wu, Z.-B.; Mak, C.-K.; Lau, T.-C. *J. Am. Chem. Soc.* **2004**, *126*, 14921.
(23) (a) Fukuzumi, S.; Morimoto, Y.; Kotani, H.; Naumov, P.; Lee, Y.-M.; Nam, W. *Nature Chem.* **2010**, *2*, 756. (b) Morimoto, Y.; Kotani, H.; Park, J.; Lee, Y.-M.; Nam, W.; Fukuzumi, S. *J. Am. Chem. Soc.* **2011**, *133*, 403. (c) Park, J.; Morimoto, Y.; Lee, Y.-M.; Nam, W.; Fukuzumi, S. *J. Am. Chem. Soc.* **2011**, *133*, 5236. (d) Park, J.; Morimoto, Y.; Lee, Y.-M.; You, Y.; Nam, W.; Fukuzumi, S. *Inorg. Chem.* **2011**, *50*, 11612.
(24) Morimoto, Y.; Park, J.; Suenobu, T.; Lee, Y.-M.; Nam, W.; Fukuzumi, S. *Inorg. Chem.* **2012**, *51*, 10025.
(25) Park, J.; Morimoto, Y.; Lee, Y.-M.; Nam, W.; Fukuzumi, S. *J. Am. Chem. Soc.* **2012**, *134*, 3903.
(26) Park, J.; Lee, Y.-M.; Nam, W.; Fukuzumi, S. *J. Am. Chem. Soc.* **2013**, *135*, 5052.
(27) (a) Fukuzumi, S. *Prog. Inorg. Chem.* **2009**, *56*, 49. (b) Fukuzumi, S.; Ohkubo, K. *Coord. Chem. Rev.* **2010**, *254*, 372. (c) Fukuzumi, S.; Ohkubo, K.; Morimoto, Y. *Phys. Chem. Chem. Phys.* **2012**, *14*, 8472.
(28) Armarego, W. L. F.; Chai, C. L. L. *Purification of Laboratory Chemicals*, 6th ed.; Pergamon Press: Oxford, 2009.
(29) Lubben, M.; Meetsma, A.; Wilkinson, E. C.; Feringa, B.; Que, L., Jr. *Angew. Chem., Int. Ed.* **1995**, *34*, 1512.
(30) *Organic Syntheses*; Saltzman, H.; Sharefkin, J. G., Eds.; Wiley: New York, 1973; Vol. *V*, p 658.
(31) (a) Lin, C. T.; Bottcher, W.; Chou, M.; Creuts, C.; Sutin, N. *J. Am. Chem. Soc.* **1976**, *98*, 6536. (b) Fussa-Rydel, O.; Zhang, H. T.; Hupp, J. T.; Leidnert, C. R. *Inorg. Chem.* **1989**, *28*, 1533. (c) Leidner, C. R.; Murray, R. W. *J. Am. Chem. Soc.* **1984**, *106*, 1606.
(32) Fukuzumi, S.; Ohkubo, K.; Suenobu, T.; Kato, K.; Fujitsuka, M.; Ito, O. *J. Am. Chem. Soc.* **2001**, *123*, 8459.
(33) Skarda, V.; Cook, M. J.; Lewis, A. P.; McAuliffe, G. S. G.; Thomson, A. J. *J. Chem. Soc., Perkin Trans.* **1984**, 1309.
(34) Kwart, H. *Acc. Chem. Res.* **1982**, *15*, 401.
(35) (a) Price, J. C.; Barr, E. W.; Glass, T. E.; Krebs, C.; Bollinger, J. M., Jr. *J. Am. Chem. Soc.* **2003**, *125*, 13008. (b) Wu, A.; Mayer, J. M. *J. Am. Chem. Soc.* **2008**, *130*, 14745.
(36) (a) Kohen, A.; Klinman, J. P. *Acc. Chem. Res.* **1998**, *31*, 397. (b) Knapp, M. J.; Rickert, K.; Klinman, J. P. *J. Am. Chem. Soc.* **2002**, *124*, 3865. (c) Klinman, J. P. *Biochim. Biophys. Acta, Bioenerg.* **2006**, *1757*, 981. (d) McCusker, K. P.; Kilnman, J. P. *J. Am. Chem. Soc.* **2010**, *132*, 5114.
(37) Fukuzumi, S.; Kobayashi, T.; Suenobu, T. *J. Am. Chem. Soc.* **2010**, *132*, 1496.
(38) (a) Parkin, G. *Acc. Chem. Res.* **2009**, *42*, 315. (b) Kotani, H.; Hanazaki, R.; Ohkubo, K.; Yamada, Y.; Fukuzumi, S. *Chem.—Eur. J.* **2011**, *17*, 2777.
(39) (a) Wolfsberg, M. *Acc. Chem. Res.* **1972**, *5*, 225. (b) Parkin, G. *Acc. Chem. Res.* **2009**, *42*, 315.
(40) Tanner, M. J.; Brookhart, M.; DeSimone, J. M. *J. Am. Chem. Soc.* **1997**, *119*, 7617.
(41) (a) Fukuzumi, S.; Ohkubo, K. *J. Am. Chem. Soc.* **2002**, *124*, 10270. (b) Fukuzumi, S.; Ohkubo, K. *Chem.—Eur. J.* **2000**, *6*, 4532.
(42) Lee, Y.-M.; Kotani, H.; Suenobu, T.; Nam, W.; Fukuzumi, S. *J. Am. Chem. Soc.* **2008**, *130*, 434.
(43) The one-electron reduction potentials of $[(N4Py)Fe^{IV}(O)]^{2+}$ (E_{red}) in the presence of acids may also have linear correlation with the quantitative measure of the Lewis acidity of acids, although the E_{red} values in the presence of other metal triflates have not been determined.[23b]
(44) (a) Marcus, R. A. *Annu. Rev. Phys. Chem.* **1964**, *15*, 155. (b) Marcus, R. A. *Discuss. Faraday Soc.* **1960**, *29*, 129. (c) Marcus, R. A. *Angew. Chem., Int. Ed. Engl.* **1993**, *32*, 1111.
(45) (a) Sutin, N. *Acc. Chem. Res.* **1968**, *1*, 225. (b) Sutin, N. *Adv. Chem. Phys.* **1999**, *106*, 7. (c) Chou, M.; Creutz, C.; Sutin, N. *J. Am. Chem. Soc.* **1977**, *99*, 5615. (d) Keeney, L.; Hynes, M. J. *Dalton Trans.* **2005**, 133.
(46) (a) Fukuzumi, S.; Honda, T.; Kojima, T. *Coord. Chem. Rev.* **2012**, *256*, 2488. (b) Fukuzumi, S.; Karlin, K. D. *Coord. Chem. Rev.* **2013**, *257*, 187. (c) Tahsini, L.; Kotani, H.; Lee, Y.-M.; Cho, J.; Nam, W.; Karlin, K. D.; Fukuzumi, S. *Chem.—Eur. J.* **2012**, *18*, 1084. (d) Yoon, H.; Morimoto, Y.; Lee, Y.-M.; Nam, W.; Fukuzumi, S. *Chem. Commun.* **2012**, *48*, 11187.
(47) (a) Takai, A.; Gros, C. P.; Barbe, J.-M.; Guilard, R.; Fukuzumi, S. *Chem.—Eur. J.* **2009**, *15*, 110. (b) Nakanishi, T.; Ohkubo, K.; Kojima, T.; Fukuzumi, S. *J. Am. Chem. Soc.* **2009**, *131*, 577. (c) Murakami, M.; Ohkubo, K.; Fukuzumi, S. *Chem.—Eur. J.* **2010**, *16*, 7820.
(48) (a) Fukuzumi, S.; Nakanishi, I.; Tanaka, K.; Suenobu, T.; Tabard, A.; Guilard, R.; Van Caemelbecke, E.; Kadish, K. M. *J. Am. Chem. Soc.* **1999**, *121*, 785. (b) Fukuzumi, S.; Mochizuki, S.; Tanaka, T. *Inorg. Chem.* **1989**, *28*, 2459.